

SOME ASPECTS OF ROCK JOINT BEHAVIOUR UNDER DYNAMIC CONDITIONS

N. BARTON

Norwegian Geotechnical Institute, Oslo.

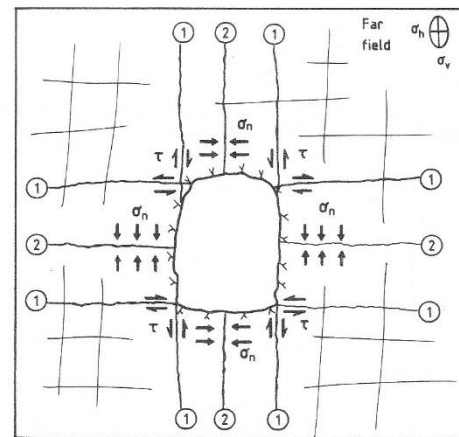
SUMMARY

Data from dynamic shear tests on rock joints are reviewed. Cyclic tests, single high velocity events, and stick-slip shear tests are included in this review. None of these tests provide an entirely satisfactory simulation of damaging dynamic loading, in which shear is accumulated in one direction during successive cycles. Case records of earthquake effects on mines and tunnels in jointed rock are discussed. Accumulation of shear, causing instability and permeability enhancement, may occur when jointing is under combined shear and normal stress. Such would be the case for steeply dipping joint structures in an anisotropic stress field, or for joints that intersect tunnel perimeters in non-radial directions. Reinforcement strategies for jointed rock subjected to dynamic loading are suggested. A method of constitutive modelling based on the JRC (mobilized) concept is suggested for modelling cyclic shear with accumulated displacement and roughness damage.

INTRODUCTION

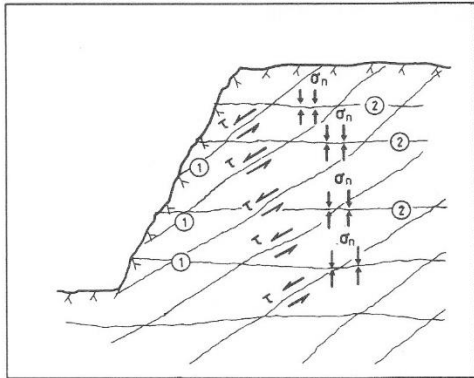
Rock joints beneath a slope or surrounding a tunnel, are acted on by shear and normal stress components. These are caused by the virgin or induced principal stresses and their relation to the orientation of the joints. If we first consider very simple examples (Figure 1) it is easy to imagine the different effects of dynamic loading. Joints that are under the influence of a shear component (τ) will tend to accumulate shear during dynamic loading, while those that are under the influence of only a normal component (σ_n) will tend to cycle (shear) back and forth.

Experimental studies designed to simulate some of the effects that can be experienced under dynamic loading are of three principal types; cyclic (shear reversal) tests, single high velocity shear in one direction, and stick-slip type experiments. The picture that evolves from a review of experimental data is somewhat confusing. Part of the problem is the difficulty of performing realistic tests. When considering the stability of the two structures illustrated in Figure 1, it is tempting to conclude that small amplitude, high frequency cyclic shear tests as often performed, will have little relevance. A shear test that accumulates shear in one direction, with limited shear reversal on each cycle would seem to be of most relevance. "Single shot", high velocity dynamic tests with shearing in only one rapid event also fall short of reality.



Idealized jointing surrounding a tunnel

Figure 1a
Predominance of normal or shear stress determines the joint behaviour under dynamic loading.



Idealized jointing beneath a slope

Figure 1b
Predominance of normal or shear stress determines the joint behaviour under dynamic loading.

BRIEF REVIEW OF DYNAMIC TEST DATA FOR SINGLE JOINTS

A shear test of a non-planar rock joint results in dilation as shear is accumulated in one direction. If we ignore asperity damage we can say that the frictional resistance will be the sum of the residual friction angle (ϕ_r) and the mobilized dilation angle (d_{mob}):

$$\phi_1 = \phi_r + d_{mob} \tag{1}$$

Upon reversal, there will be a form of "sliding downhill", and frictional resistance in certain circumstances could be approximated as follows:

$$\phi_2 = \phi_r - d_{mob} \tag{2}$$

1. Reversed Shear and Cyclic Shear Tests

Three sets of data that include reversal are shown in Figures 2, 3 and 4. The initial shear stress displacement and dilation record shown in Figure 2 indicates

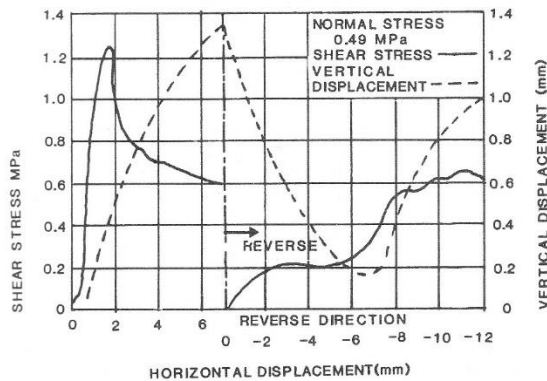


Figure 2
Direct shear data for joint in weathered greywacke, after Martin and Millar (1984). Note contraction on reversal, and remobilization when passing origin.

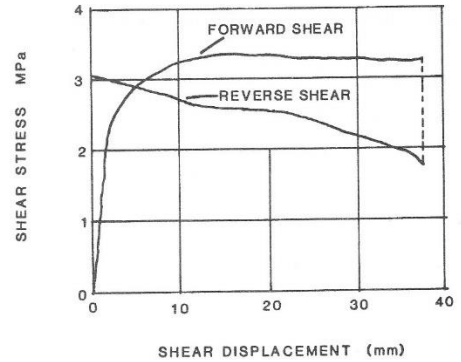


Figure 3
Reversed joint shear under a normal stress of 4.1 MPa, after Weissbach and Kutter (1978).

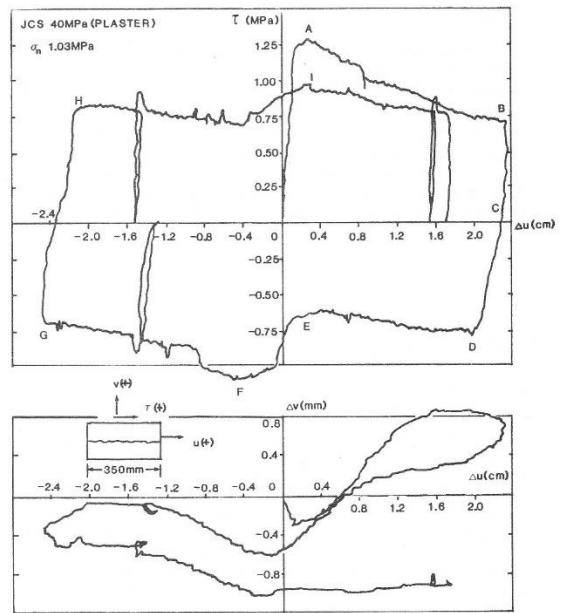


Figure 4
Multiple reversal shear test showing shear stress-displacement and dilation records for a plaster replica of a joint in sandstone, after Celestino and Goodman (1979).

that dilation is incomplete after 7 mm of shear. Reversal of the shear direction at this point causes contraction and a markedly slower mobilization of shear strength in the reverse direction (due to $\phi_r - d_{mob}$ effect). However, on passing the "origin" after 7 mm of reversed shear, dilation increases, and shear strength is mobilized, but to little higher than the original level.

Figure 3 indicates a similar ($\phi_r - d_{mob}$) effect, caused by contraction upon reversal. Weissbach and Kutter (1978) suggested that the midpoint of the stress drop should give an accurate value of ϕ_r , in this case approximately 31° ($\arctan 2.5/4.1$).

One of the earliest complete shear reversal records apparently available in the literature is reproduced in Figure 4 from Celestino and Goodman (1979). Unfortunately, Celestino and Goodman's data were not obtained directly from rock joints, there was no weathering effect to stimulate gouge production, and the roughness of the surfaces was unusual, consisting of interlocking ripple marks molded from joints in sandstone.

Numerous shear reversal records are reported by Gillette et al., (1983), but the data was obtained from rapidly cycled tests with frequencies in the range 0.1-1 Hertz. Their shear displacements were limited in most cases to 2 mm or less for a sample length of 200 mm. Conventional post-peak behaviour was not apparent in the results, although the samples were of course gradually worn smooth by the reversals. In fact, many of the specimens reportedly became cherry red hot and some regions experimented metamorphism at the higher normal stress levels, when frequencies of 1-10 Hz were applied, and after several hundred cycles.

So-called shearing "rate effects" have also been studied in detail by Crawford and Curran (1981). Their data has been expressed in dimensionless form by Gillette et al. (1983) as shown in Figures 5 and 6.

In essence, their work indicated that the softest rock (dolomite) exhibited an increase in shear resistance with increasing shearing rate, especially at low normal stress. At higher stress levels the strength tended to be lower with increasing rate. Intermediate-hardness rocks such as granite exhibited imperceptible rate-effects. The two hardest rocks, syenite and sandstone, essentially reduced in strength. It should be carefully noted that all the specimens tested by Crawford and Curran were sawn (ϕ_b -type) rock surfaces.

The rate-effect tests shown in Figure 6 for tension fractures in a low to medium hardness sandstone demonstrate a consistent increase in shear strength beyond a shear velocity of 0.1-1 mm/s. The fact that these surfaces were non-planar means that they would exhibit all three strength components according to the Barton and Choubey (1977) description of frictional strength:

$$\phi = \phi_r + JRC \log(JCS/\sigma_n) \quad (3)$$

where ϕ = peak friction resistance
 JRC = joint roughness coefficient
 JCS = joint wall compression strength
 σ_n = effective normal stress

Since the roughness (JRC) is not going to alter with rate of shear, the components ϕ_b and JCS separately, or in combination, must be exhibiting the rate effect. It has been shown by Barton (1976) that (JCS) in equation 3 can be replaced by the confined strength ($\sigma_1 - \sigma_3$) when asperities are confined under higher stress levels. A consistent increase in ($\sigma_1 - \sigma_3$) with loading rate is apparent from data collected by Brace and Jones (1971) and reproduced in Figure 7. It is therefore reasonable to expect that the shear resistance of non-planar joints will exhibit a minor increase with increased loading rates.

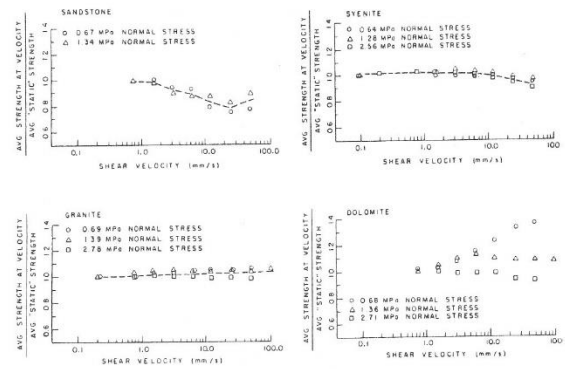


Figure 5 Dimensionless rate-effect shear strength data from tests by Crawford and Curran (1981) as derived by Gillette et al. (1983). All samples were sawn surfaces, i.e. exhibiting ϕ_b -type behaviour.

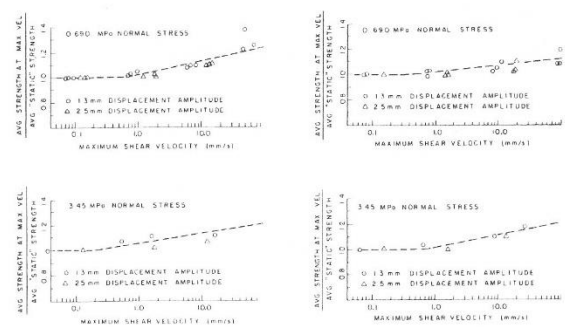


Figure 6 Results of rate dependent shear tests on two tension fractures in sandstone. The results are derived from cyclic shear tests, after Gillette et al. (1983).

An experimental difficulty with cyclic, multiple reversal, shear tests is that shear debris or gouge produced by the back-and-forth shearing is difficult to contain within the joint plane (Plesha and Haimson, 1988). "Seating" or negative bulking may therefore be experienced. Since positive or negative dilation affects shear strength (equations 1 and 2) the resulting shear resistance may also be affected. A joint in situ will not "lose" gouge material in this way. An experimental result that reveals this "seating" is shown in Figure 8.

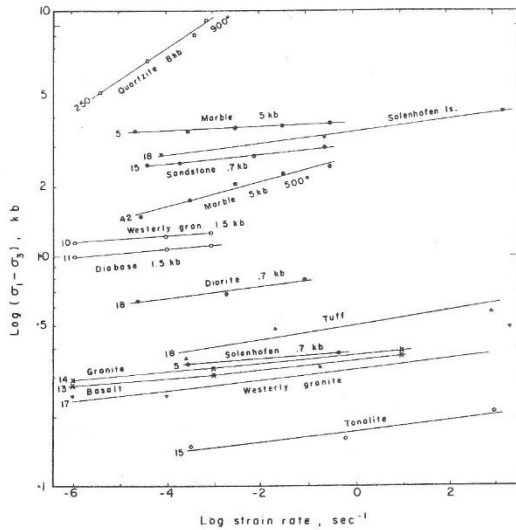


Figure 7
Influence of strain rate on confined compression strength, after Brace and Jones (1971).

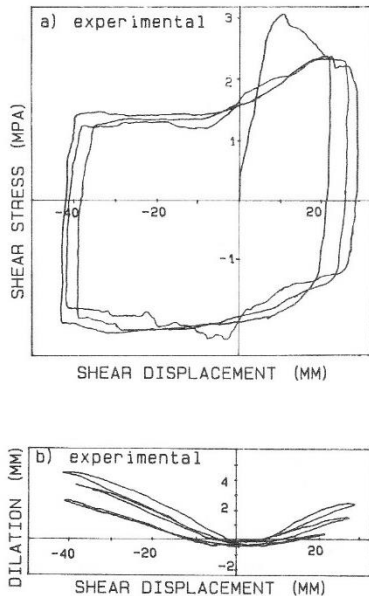


Figure 8
Experimental and numerical results for cyclic direct shear test, Kutter and Weissbach (1980).

2. Length of Stick, Shearing Rate, and Creep

Experiments reported by Dieterich (1972) on rough-ground surfaces of sandstone, quartzite, graywacke and granite have indicated that accumulations of powdered rock debris on a shear surface exhibit strongly time-dependent properties. Static friction increases with the logarithm of the time that adjacent blocks remain in stationary contact. Over the range of normal stresses from 2-85 MPa, the coefficient of static friction ($\arctan \tau/\sigma_n$) for 10⁵-s intervals between stick-slip events is 6-10% greater than for 15-s intervals. These results appear to be dependent both on the presence of gouge and on periods of stick, rather than on slow shear rates, since Byerlee and Brace (1968) found no detectable variation in frictional strength over a wide range of strain rates.

The compilation of data for differential stress ($\sigma_1 - \sigma_3$) at a failure over as many as nine log cycles of strain rate (10⁻⁶ - 10³ per sec) given by Brace and Jones (1971) does indicate about 5% increase in strength per log cycle of strain rate (Figure 7). A corresponding increase in JCS at typical tunnel depths represents only about 1/20 increase in peak friction per three log cycles of strain rate, which confirms Byerlee and Brace's (1968) results.

Dieterich's results are clearly important for any fault surfaces in the neighbourhood of a deep tunnel, but the question arises whether they need to be considered for the case of essentially gouge free, undisplaced joints. Tests by Dieterich (1972) and Hoskins et al. (1968) on rough, clean rock surfaces showed stable sliding characteristics. It appears that a degree of polish and/or gouge is required before stick-slip mechanisms take over from stable sliding. There are also indications that increased temperature also increases the range of stable sliding (Brace and Byerlee, 1970).

Rough, clean surfaces such as relatively undisplaced rock joints will apparently not be subject to significantly increased shear strength with increased duration of stationary contact.

The effect of long-term loading on the creep experienced by unfilled rock joints was studied by Schwartz and Kolluru (1982), using a gypsum-based model material with an unconfined compression strength of 26 MPa. The "joints" were simulated with flat sanded, saw-cuts, i.e. the surfaces were essentially exhibiting ϕ_b properties only. The authors found that the magnitude of shear strain depended to some extent on the ratio $\tau/\tau(\text{peak})$ where τ = the applied shear stress, but depended most strongly on the level of normal stress.

3. Single shot, high velocity shear tests

Bakhtar and Barton (1984) describe a large scale series of nineteen shear tests performed on fractures 1.0 m² in area, generated in blocks of sandstone, granite, tuff, hydrostone and concrete. The tests were conducted under quasi-static and dynamic loading conditions. A stress assisted tensile fracturing technique was developed to create the fractures through the large test blocks. Prior to testing, the fractured surface of each block was characterized using the JRC-JCS concept. The results of characterization were used to generate the peak strength envelope for each fractured surface.

The quasi-static (slow rate) shear tests were performed in a large biaxial test frame, the fracture making a diagonal. Single direction shear velocities in the range 0.001-0.1 mm/sec were used in the static tests, while the dynamic tests had shear velocities in the range 400-4000 mm/sec using a gas loaded cylinder. Peak loads as high as 260 tons and a rise time of 90 milliseconds produced peak accelerations up to 60 g.

Prior to testing in pseudo-static or dynamic shear, each fracture or saw cut was characterized by performing: 1) tilt tests for JRC, 2) Schmidt hammer tests for JCS, 3) tilt tests for ϕ_b , and 4) roughness profile measurements. The data obtained was used as input in a joint behaviour model to predict: peak shear strength envelope (τ , σ_n) and dilation (d_n) due to JRC(mobilized). The latter was used to correct the theoretical (transformed) stress path to allow for out of plane shear (at angle $\beta+d_n$).

In general, utilization of the characterization data and the above dilation correction allowed Bakhtar and Barton (1984) to predict the subsequently measured strengths to an accuracy of $\pm 15\%$. When the tests were partitioned as pseudo-static or dynamic, the average predicted shear strengths were approximately 5% lower than measured under pseudo-static conditions, and 10% lower than measured under dynamic conditions. By implication, the joint behaviour model was slightly conservative, and the dynamic strength may be some 5% higher than the static strength when shear displacement velocities of approximately 0.001-0.1 mm/sec (pseudo-static) are compared with the dynamic velocity range of approximately 400-4000 mm/sec.

A review of test data indicates that the unconfined compressive strength of rock does increase significantly as loading rate is increased. For example,

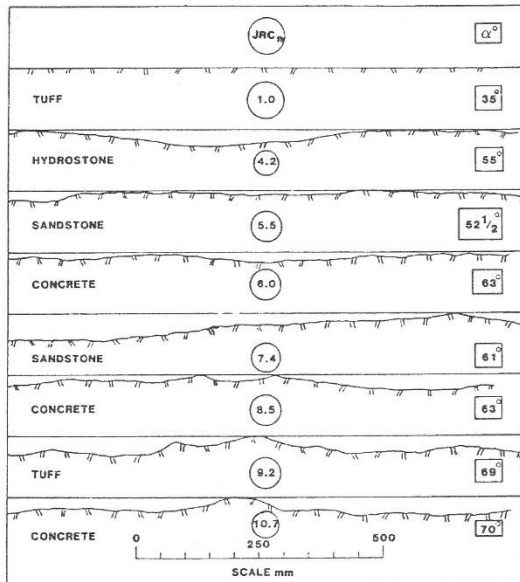


Figure 9 Fracture surface profiles, tilt angles (α) and large scale roughness coefficients (JRC_n) of samples. (Barton and Bakhtar, 1984).

tests reported by Green and Perkins (1968) indicate approximately 40% increase in σ_c (unconfined) when the strain rate is increased from about 10^{-4} sec^{-1} to 10^3 sec^{-1} .

Under conditions of shear loading the test results indicated only minor rate effects (approximately 5%) when shear velocities were no more than 1-4 meters per second. The cyclic shear loading tests reported by Gillette et al. (1983) for tension fractures in sandstone indicate that rate dependence is probably absent until velocities exceeding 1 mm/second are reached. Between 1 mm/sec and 100 mm/sec an increase in shear strength of 10-15% was indicated. However, it is not known exactly how comparable rate effects obtained from cyclic loading will be, compared to the single pulse, unidirectional shear events.

Figure 9 illustrates the roughness profiles and tilt angles measured for the large blocks tested by Bakhtar and Barton (1984). Average joint characterization data for the rock materials and surfaces tested are given in Table 1.

Table 1 Average Laboratory and Full-Scale Shear Strength Parameters Obtained in the Study by Bakhtar and Barton (1984)

Laboratory Scale	Full-Scale
JCS ₀ = 52 MPa	JCS _n = 30 MPa
JRC ₀ = 7.9	JRC _n = 5.6
$\phi_r = 32^\circ$	$\phi_r = 32^\circ$

For illustrative purposes the above average values will be utilized to demonstrate the approximate differences that are obtained when laboratory data is used to predict shear strength in place of in-situ scale data. We will further demonstrate the effect on in-situ shear strength that is predicted, if a 50% increase in intact rock compressive strength is assumed to occur as a result of dynamic loading. Three effective normal stress levels will be utilized: 1 MPa, 10 MPa and 30 MPa. The results shown in Table 2 demonstrate that the parameters affecting shear strength can be classed in order of importance as follows:

- First Order -- normal stress level
- Second Order -- scale effect
- Third Order -- dynamic loading

Table 2 Demonstration of Scale Effects and Dynamic Load Effects

Normal Stress	Laboratory Scale (Static)		In-Situ Scale (Static)		In-Situ (Dynamic)	
	τ (MPa)	ϕ (peak)	τ (MPa)	ϕ (peak)	τ (MPa)	ϕ (peak)
1 MPa	1.02	45.6°	0.85	40.3°	0.88	41.3°
10 MPa	7.72	37.7°	6.92	34.7°	7.18	35.7°
30 MPa	20.15	33.9°	18.75	32.0°	19.47	33.0°

A dynamic event causing an increase in normal stress will obviously result in a very large increase in shear resistance. If, for some reason, the dynamic event left the normal stress level unchanged, then little increase in shear strength could be expected. The 50% increase in compressive strength assumed above results in only 3-4% increase in peak shear strength, due to the logarithmic dependence of the friction angle on the ratio of JCS/σ_n .

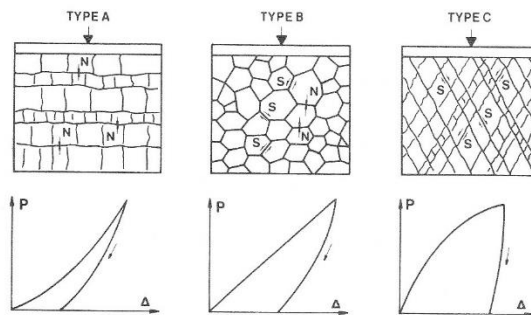
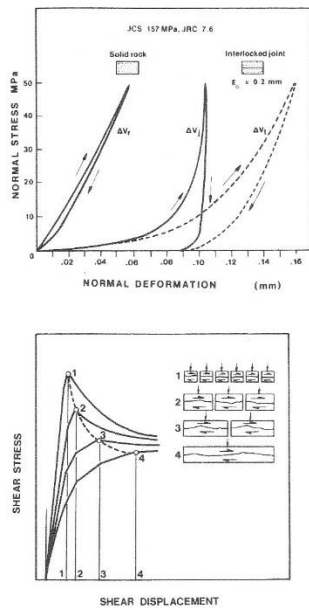


Figure 10 Normal and shear deformation components for single rock joints (Bandis et al. 1981, 1983) and their influence on rock mass deformation (Barton, 1986).

ASPECTS OF DYNAMIC LOADING OF ROCK MASSES

Dynamic loading of rock masses obviously involves combinations of normal and shear load cycling for the individual joints affected. We have seen the manner in which shear unloading occurs (see Figures 4 and 8). Bandis et al. (1983) have shown how joints unload in a normal sense.

1. Deformation components in a rock mass

The combination of these load-unload characteristics for three hypothetical rock masses are shown in Figure 10. Dynamic loading effects when the principle dynamic wave component is travelling vertically will tend to result in the rock mass deformation characteristics given in Table 3.

Table 3 Three Characteristic Load-Deformation Behaviours for Rock Masses

Type	Dominant Mode	Shape	Hysteresis	Lateral expansion
A	Normal	Concave	Small	Small
B	Normal and shear	Linear	Moderate	Moderate
C	Shear	Convex	Large	Large

Inversible effects increase for the case with the joints that are predominantly non-parallel and non-perpendicular with the principal stress or loading direction. These can be expected to accumulate shear in the same way as the joints labelled (1) surrounding the tunnel or rock slope in Figure 1.

2. Pore Pressure Hardening Effects Due to Aperture Strain

A factor that some experimenters have considered in their tests on single rock joints is the potential change in pore pressure or joint water pressure as a result of dynamic loading. For example, Gillette et al. (1983) monitored the shear displacement and joint water pressure during numerous load cycles. They found that significant joint water pressure increases occurred during undrained cyclic loading, leading to a state of nearly zero effective stress. This observation, similar to that for sands, is surprising for a low porosity rock, and may perhaps reflect loss of gouge material with successive cycles.

Intuitively, shearing of a tightly interlocked non-planar joint will result in dilation and an initial reduction in pore pressure if the shearing rate exceeds the rate at which water can flow into the dilating sections of the joints. This problem is experienced when dredging of rock under water. The chips of rock that are developed by the dredger-wheel teeth, resist shearing and removal more strongly if the water depth is increased or if the wheel's rotation speed is too high. The reasons for this are significant.

A joint that is sheared too fast compared to its drainage capacity will be subjected to an effective normal stress equal to the overburden (in this case

water) plus the one atmosphere of vacuum created by the cavitation. Increased water depth therefore increases the frictional existence as described by equation 3.

It is possible to generate shear strength-displacement, dilation-displacement, and conductivity-displacement diagrams for the above problem (Barton and Bakhtar, 1984). Displacement of the chip of rock at a certain shearing rate is used to calculate the incremental change of effective normal stress as drainage of pore water occurs at each end of the rock chip.

We can draw some parallels between this problem and the idealized rock slope illustrated in Figure 1. Let us suppose that the slope is a very large open pit and that it is loaded by an earthquake with larger horizontal than vertical acceleration components. A hypothetical set of shear strength-displacement, dilation-displacement and conductivity-displacement diagrams for the slope are given in Figure 11 for the following assumed rock joint characteristics:

$$\begin{aligned} JRC_0 &= 10 && \text{(small scale roughness)} \\ JCS_0 &= 100 \text{ MPa} && \text{(small scale wall strength)} \\ \phi_r &= 30^\circ \end{aligned}$$

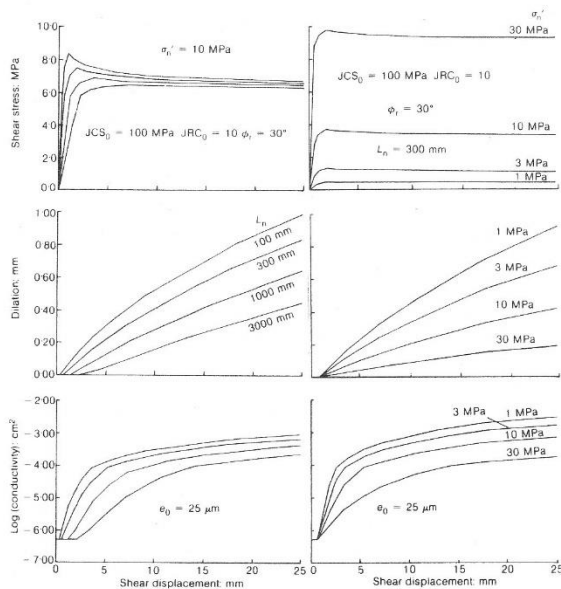


Figure 11
Hypothetical joint behaviour curves for joints in the walls of a large open pit. Note influence of block size and normal stress.

Various block sizes are assumed in generating the sets of curves shown in the figure. The scaling method is described by Barton and Bakhtar, (1982). An assumed initial joint conducting aperture (e) of $25 \mu\text{m}$ has been assumed for all joints for simplicity, although in practice the joint apertures might vary from perhaps $100 \mu\text{m}$ to $10 \mu\text{m}$ over the stress range of 1 MPa to 30 MPa for this hypothetical 1000 m high pit slope.

The large dimensions of the slope are comparable to seismic wave lengths and entail the risk of simultaneous in-phase acceleration of large parts of the slope. This contrasts with the tunnel problem illustrated in Figure 1, which will not suffer distress with low frequency long wave length earthquake waves, but might show irreversible shears following high frequency blasting.

Examination of the dilation and conductivity curves in Figure 11 indicate that joints nearer the surface may undergo "pore pressure hardening" if shearing of joint set (1) exceeds 1 to 3 mm (variation due to block size). If the shearing occurs more rapidly than a joint of 10^{-6} to 10^{-4} cm^2 conductivity can drain water towards itself, then the effective normal stress can be expected to increase by up to 0.1 MPa. Such a moderate effect can be expected to stiffen only the upper parts of the slope. The risk (if shearing does occur despite hardening) is that any water that has flowed into the dilated zones will be only partially expelled in the next shear reversal, and could cause a much larger reduction of effective normal stress than the 0.1 MPa increase on the first forward shearing event.

EARTHQUAKE LOADING OF UNDERGROUND STRUCTURES IN JOINTED ROCK

Underground structures have a consistent record of suffering much less damage than surface facilities during earthquakes. Generally only portal areas or fault crossings have suffered severe damage. In the case of portals, the combination of poor ground, stiff linings and amplified near surface shaking, make earthquake resistant design very difficult.

The reduced intensity of shaking experienced at depth and in more competent rock masses, appear to limit damage to occasional rock drops and to cracking of linings. These events may be the result of out-of-phase high frequency shaking, reactivation of joint slip, or positive or negative stress changes adversely affecting existing high or low stress conditions.

In each of these cases the net result may be partially irreversible strain, due to the hysteretic behaviour of jointed rock masses. As suggested above, the impact on stability may be minimal, but the secondary effect on coupled processes such as water inflow or leakage may be marked. Seemingly minor joint displacements can cause radial changes in conductivity.

The present international interest in geological disposal of high level nuclear waste has focussed particular attention on transport velocities through jointed media. Since migration of radionuclides via ground water flow is the only conceivable mechanism for release to the biosphere, any events that could cause radical changes in flow velocities are of potential concern. Reports describing mine flooding and cracking of linings as a result of earthquakes are indications of a potential problem that may have increased impact on design in the future.

A number of references to mine flooding or increased flows of water as a result of earthquakes are given in the literature. There are also occasional references to greatly diminished flows. Unfortunately details are seldom given on the exact cause of the flooding, whether one or several levels or an entire mine were subject to flooding. A tabulation of earthquake

effects on tunnels and mines given by McClure (1982) provides comments such as "mine filled with water", "mine was flooded", "existing fractures were opened wider causing increase in water influx and almost flooding mine". Two of these cases were in California, one was in Chile.

Stevens (1977) suggested that in such cases the earthquakes may have resulted in renewed movement along existing fractures, or that fracturing resulted from the earthquake and provided new avenues for water inflow into the mines.

A recent earthquake in Idaho (2 November 1983) registering 6.9 on the Richter scale caused damage to hundreds of buildings and two fatalities. It also caused a 350% increase in water flow into the 1100 ft deep Clayton silver mine. The mine is located 25 miles west of the epicentre. Flow increased immediately from 1000 gal/min to 2500 gal/min but declined over a six-month period to about 1500 gal/min (Rovetto, 1984).

Flow rates and pressures reportedly increased in numerous locations in the 800 ft and 1100 ft levels, while the 500 ft level produced water for the first time in several years. Major jointing in the local quartzite and dolomite strikes approximately north-south and dips at about 60°. Inflowing water remained clear following the earthquake.

This case is an example of joint conductivity enhancement, rather than fault displacement effects. Furthermore, dynamic stress cycling that occurs only perpendicularly to the joints is unlikely to cause significant increase or decreases in aperture and conductivity if the joint is already under significant levels of effective normal stress. The essentially permanent change in aperture must have been caused by shear-induced dilation across non-planar joint surfaces. Reversed shear and contraction on subsequent cycles of shaking will be inhibited if a significant level of differential stress already exists. The subsequently reduced flows observed in the Clayton silver mine are probably a function of local drawdown of the groundwater table due to the increased permeability of the rock mass.

Locations having high ratios of principal stress in combination with obliquely dipping persistent jointing will be least able to resist seismic loading due to the likelihood of high shear stress components. A high virgin level of shear stress, perhaps locally accentuated by excavation, would provide the unwanted driving force for progressive, irreversible accumulation of shear displacement during seismic shaking.

As regards rock reinforcement strategies, it is interesting to observe from Figs 11a and 11b that, if shear displacement are controlled, changes in permeability can be reduced to a minimum. For example, slip magnitudes of only 1 mm will mobilize the majority of available shear strength but will not be sufficient to cause marked dilation or changes in conductivity, i.e. a rock reinforcement system that is successful in limiting individual joint displacements to the range 0-1 mm will optimize stability and minimize conductivity changes. A flexible lining such as mesh or fibre-reinforced shotcrete might also tolerate such displacements without cracking. Increased leakage or inflow problems would probably not develop at these levels of shear displacement.

Once this threshold of 0-1 mm displacement is passed, shotcrete and concrete linings will tend to crack, shear and dilate, and the conductivity of the features behind the cracks may increase dramatically, probably by an order of magnitude in the first 10 mm of shear.

A review of damage to tunnels caused by earthquakes by Dowding and Rozen (1978), reveals that unlined tunnels generally do not experience any block falls until peak surface accelerations and velocities exceed about 0.2 g and 20 cm/sec respectively. A few incidences of minor cracking occur in concrete lined tunnels between 0.25 g and 0.4 g. Severe damage involving major rock falls or severe cracking appears when peak surface accelerations and velocities exceed 0.5 g and 80 cm/sec, and then mostly in poor ground or in portal areas. Total collapses occur when tunnels are intersected by faults that displace during the shaking.

Experimental tunnels located in the immediate neighbourhood of underground explosion tests have also indicated a range of damage, from occasional rock falls in unlined tunnels (average $v = 120$ cm/sec, minimum $v = 46$ cm/sec), to cracking ($v = 90$ cm/sec) and faulting ($v = 120$ cm/sec) of the shotcrete in tunnels that are bolted and shotcreted. However, in blasting tests, peak particle velocities and accelerations occur at frequencies of about 20-200 Hz, whereas peak earthquake motions normally occur at between 0.5 and 10 Hz. The much longer wave lengths of earthquakes (hundreds to thousands of metres) are much less likely to cause differential displacements across the tunnels than blasting. Even large span openings are small in comparison to these wave lengths, and differential displacements across them should be insignificant.

PHYSICAL MODELS OF DYNAMIC JOINT BEHAVIOUR

The processes occurring in a rock mass during dynamic loading are of course very complex. Physical models with idealized jointing and simple structures give some insight into the dynamic behaviour of the joints, and illustrate some of the phenomena we have referred to earlier.

Two-dimensional, plane stress models of large near-surface excavations were performed in a joint Norwegian-Swedish study of underground siting for nuclear power plants reported by Barton and Hansteen (1979). The models consisted of a weak, brittle rock simulant, which was divided into 20,000 discrete blocks by two intersecting sets of tension fractures. Four different fracture (joint) orientations were studied, and models of single caverns, two parallel caverns, and four closely spaced caverns were tested.

Physical excavation of the caverns took place after the model rock masses had been fully consolidated with four load-unload cycles, and while they were under either hydrostatic or high horizontal stress. The models were dynamically loaded after excavation, while still under stress. Deformation vectors were generated by photogrammetric analysis in a stereocomparator linked to a computer and plotter.

The dynamic response of the model rock masses to simulated earthquake loading was recorded by two miniature accelerometers. These were buried at simulated depths of approx. 20 m below the surface. Peak horizontal components of motion, which were 4-5 times the vertical, were as follows at prototype scale:

$a = 0.2 - 0.7 g$, $v = 15 - 90 \text{ cm sec}^{-1}$,
 $s = 6 - 30 \text{ cm}$, $t = 0.4 - 12 \text{ Hz}$
 duration = 1 min

The deformation occurring during this dynamic loading was dependent on three factors: the orientation of the joints, the ratio of horizontal to vertical stress, and the depth below surface. Progressive collapse of walls and pillars occurred in the models with unfavourable, steeply dipping joints. None of the excavations were supported or reinforced in any way.

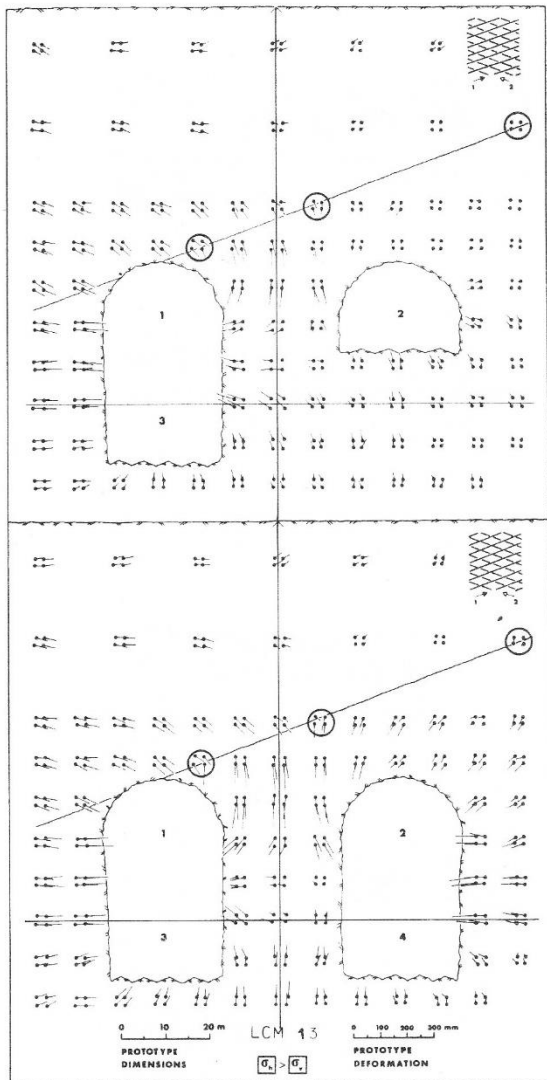


Figure 12
 Progressive joint slip caused by physical model excavation in a high horizontal stress field, Barton and Hansteen (1979).

Figure 12 illustrates the deformation vectors measured during excavation of simulated 25-m span caverns. The width of field shown in the figure is less than one sixth of the whole model; boundaries were distant. The shallow-dipping jointing (shown at the correct relative scale) in combination with the high horizontal stress resulted in slip on one of the joints that intersected the roof of the left-hand cavern. The order in which excavation was performed is shown by the numbers 1-4.

Slip could not be detected after stage 1, but it could be detected after stage 2, and it then increased progressively through to stage 4. The three circles illustrate the vectors measured at reference points straddling the slipping joint. While the major deformation vectors are directed towards the openings, a slip component of at least 50 mm is indicated at prototype scale.

In Figure 13 the net effect of dynamic loading is shown, with each group of four vectors drawn from the mean position. Settlement, increased deformation towards the openings, and additional joint slip are evident. The divergence of the vectors shown circled indicates additional relative slip of 40-80 mm (full scale) as a direct result of the simulated earthquake loading. This would be sufficient to cause major additional increases in conductivity.

Several other features are illustrated by these physical models. While there was settlement above the openings, little was evident below them. Deformation tended to occur upwards towards the excavations, despite the 150 m of simulated rock mass beneath them. In general the zone around the openings that was sensitive to dynamic loading was more or less the same zone that suffered deformation during excavation.

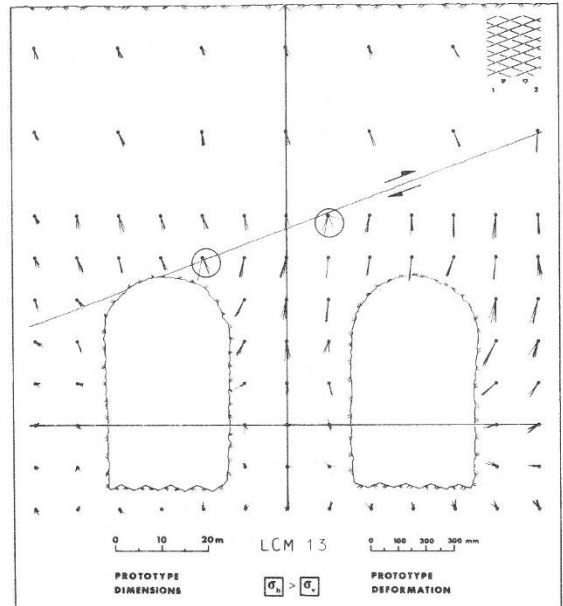


Figure 13
 Net deformation caused by simulated earthquake loading of the physical model, after excavation.

The disturbance of the virgin stress caused by excavation causes a sufficient increase in the ratio τ/σ_n along individual joints (due to increased shear and reduced normal stress) that they are locally susceptible to progressive accumulation of shear displacement (fatigue) from a small number of cycles. The number of cycles required to cause settlements in the undisturbed model rockmass would be far in excess of the few tens of significant cycles resulting from the model earthquakes.

Cyclic compressive loading tests performed on jointed models by Brown and Hudson (1974) led these authors to

conclude that rock masses were unlikely to be susceptible to fatigue when loaded at low ratios of stress to strength. In the models illustrated in Figures 12 and 13 the joints were under quite high ratios of shear stress to shear strength due to high initial stress anisotropy and subsequent excavation. They were therefore susceptible to irreversible, progressive accumulation of slip after relatively few cycles. Figure 14 demonstrates how block falls develop progressively during shaking. These events do not occur immediately shaking begins, but require some tens of cycles to develop.

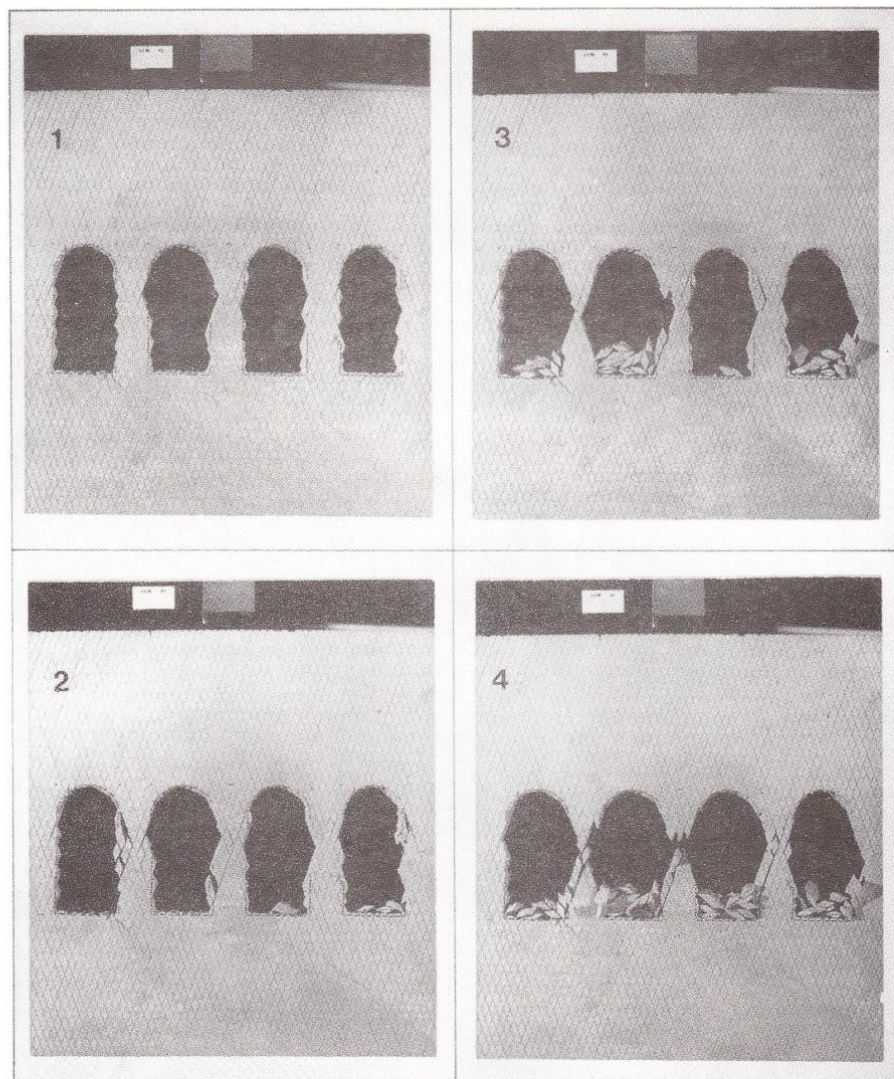


Figure 14
Progressive collapse of walls and pillars when jointing is unfavourable. Several tens of cycles of shaking are required. (After Barton and Hansteen, 1979).

DYNAMIC DESIGN STRATEGIES FOR TUNNELS

From the foregoing review of real and simulated seismic effects on tunnels, it appears feasible to suggest some general design strategies. It appears obvious that locations having high ratios of principal stress in combination with obliquely-dipping persistent jointing, will be least favourable, due to the likelihood of high shear stress components and potentially low shear strength. This will depend on the degree of joint roughness and on the persistence.

A high virgin level of shear stress, locally accentuated by excavation, would provide the unwanted driving force for progressive, irreversible accumulation of shear displacement during seismic shaking. If such sites are unavoidable, but cavern orientation can be varied, then a perpendicular between the excavation axis and the strike of these persistent joints would be advisable both from stability and conductivity-enhancement considerations. Optimistically this orientation would also place the principal horizontal stress perpendicular to the excavation axes, if as is often the case, the persistent jointing was parallel to the principal stress direction.

Reinforcement for dynamically loaded joints

The use of a general rock mass reinforcement and tunnel support method such as the Q-system will not be appropriate in cases where adverse jointing defines deep unstable wedges, or where potential motion on a fault has to be tolerated by the reinforcement. Such cases warrant special design and should incorporate appropriate bolt orientation angles, and bolt stiffnesses that are consistent with the strength-deformation properties of the geological feature being secured.

Direct shear tests performed on bolted blocks or jointed rock indicate peak shear resistances when the bolt forms an acute angle of about $35-50^\circ$ from the plane of the joint, and is under tension rather than compression. The bolt tension contributes an increase in normal stress, thereby enhancing the shear strength. The range of angles ($35-50^\circ$) corresponds to the mobilized friction angle which may be pre- or post-peak according to the shear displacement reached when the maximum combined shear resistance is reached.

A similar bolt orientation in a tunnel intersected by a persistent set of joints will be successful only if the bolts have high enough capacity to prevent large post-peak displacements from occurring. As indicated in Figure 11 the bolts would need to be stiff enough (fully grouted) and of high enough capacity (large cross-sectional area of high strength steel) to prevent displacements larger than 1-3 mm from occurring.

Small displacements may be difficult to guarantee during a major earthquake, and some flexibility in the bolting may need to be designed: for example by grouting only the ends of the bolts. When such a design is contemplated the appropriate post-peak, pre-residual shear strength - termed the mobilized strength - will need to be estimated to ensure optimum orientation of the bolts.

In the force diagram illustrated in Figure 15 a major unstable wedge in the right wall of a large tunnel or open pit is assumed. The wedge has a total weight represented by the force (W), an uplift force (U) from water pressure in the adversely dipping joint, and an outward-directed force (T) from an assumed worst-case

water pressure acting in a secondary joint which forms a potential tension crack through the upper part of the wedge. Additional forces representing the components of peak seismic acceleration acting on the wedge would be added to the force diagram, at the position shown in the figure.

Closure of the force diagram and calculation of the bolting capacity needed to ensure an adequate factor of safety is achieved by constructing the appropriate strength envelope using the joint perpendicular (dotted line) as the axis of effective normal stress. The frictional resultants (R_r , R_m and R_p) are oriented according to whether design is based on residual, mobilized or peak strength and displacement respectively.

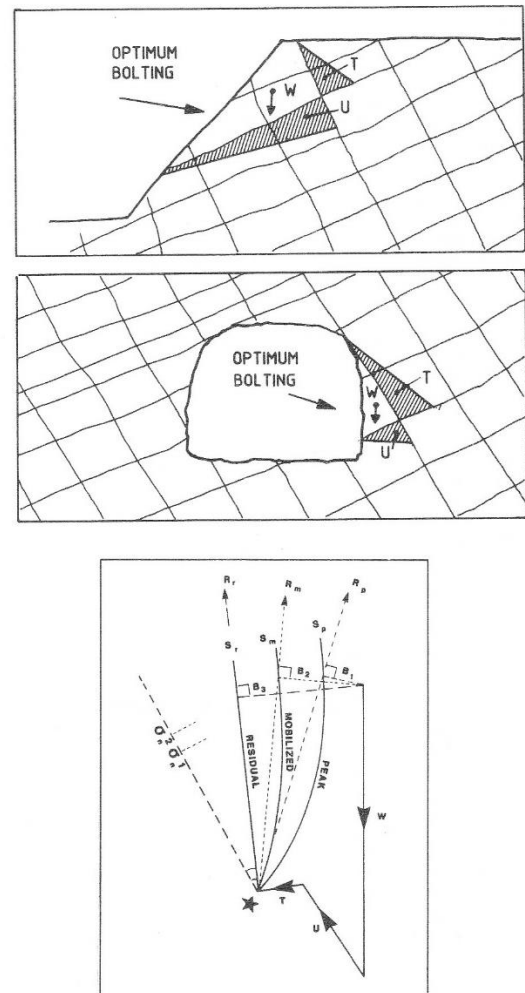


Figure 15
Optimum bolt installation angles and load capacities for dynamic loading will vary with the amount of shear displacement allowed. (Add dynamic components Wfg at point *).

The bolt forces required for equilibrium (B_3, B_2 or B_1) are dimensioned and oriented accordingly. Note that moment equilibrium is satisfied only if the above forces pass through the centroid of the wedge. This is unlikely, but associated errors are acceptably small.

A CONSTITUTIVE MODEL FOR CYCLICALLY LOADED JOINTS

The foregoing discussion of dynamic loading effects on tunnels has focussed on the "accumulation" of joint shear displacement, as the mechanism that must be resisted by suitable reinforcement. In many dynamic loading situations, the accumulation of shear displacement will be the sum of larger forward and lesser reverse displacements. If we consider the idealized rock slope in Figure 1 it is easy to recognise that displacement in a forward direction (towards the excavation) will be accumulated in a smaller number of cycles, if the dip of joints labelled (1) is steeper than shown. A shallower dip will increase the number of cycles required to reach "failure", however that is defined.

The cyclic shear test behaviour shown in Figures 4 and 8 need to be modelled in a manner that allows accumulation of shear and associated damage, if such events are to be numerically simulated. A step in this direction can be made by considering the mobilization of roughness with increased shear displacement.

The friction angle (ϕ_{mob}) mobilized at any given displacement δ can be expressed by the following general equation

$$\phi_{mob} = JRC_{mob} \log(JCS/\sigma_n') + \phi_r \quad (4)$$

where JRC_{mob} is the mobilized roughness and σ_n' is the effective normal stress.

The following key aspects of shear behaviour can be modelled in the order in which they occur during a shearing event (see Figure 16).

- (a) Friction is mobilized when shearing begins.
- (b) Dilation begins when roughness is mobilized.
- (c) Peak shear strength is reached at $JRC_{mob}/JRC_{peak} = 1.0, \delta/\delta_{peak} = 1.0$.
- (d) Dilation declines as roughness reduces.
- (e) Residual strength is finally reached.

The (i) component shown in an inset to Figure 16 has both a geometric component (JRC) and a cohesive component (JCS/σ_n'). In the example shown in Figure 16, the value of $JRC(mob)$ in equation 4 has been normalized by division by $JRC(peak)$. The origin of the dimensionless plot in Figure 16 is given by the y-coordinate ($-\phi_r/i$) and is therefore stress dependent. A different shape of curve is produced when the ratio of JCS/σ_n' is changed.

The test parameters reported by Celestino and Goodman (1979) indicate that the value of ($-\phi_r/i$) will be approximately -2 for the example shown in Figure 4. This gives a convenient initiation point for converting the data to the form $JRC(mob)/JRC(peak)$ and $\delta/\delta(peak)$ as in Figure 16.

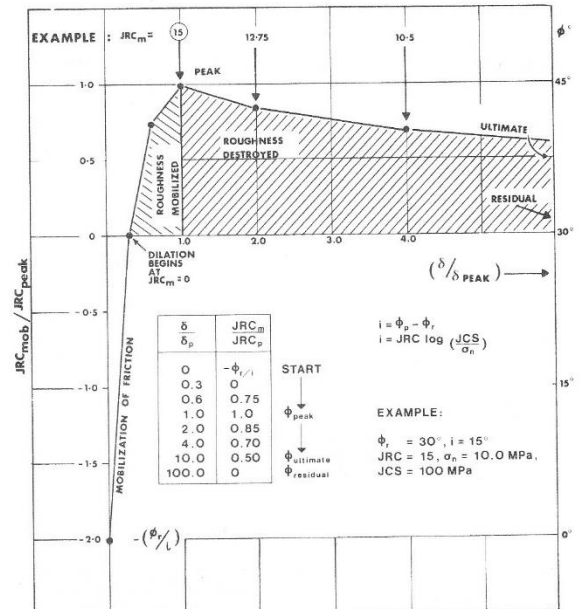


Figure 16 Dimensionless model for shear stress-displacement modelling, after Barton (1982). In this example $\phi_r/i = 2$.

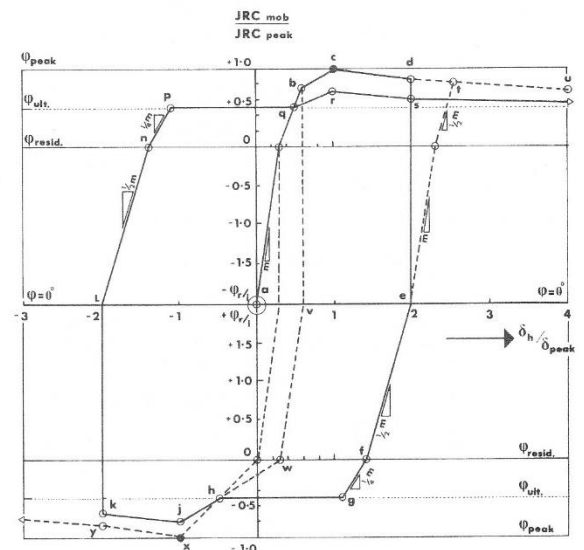


Figure 17 A preliminary model for simulating the effects of cyclic shear and accumulated shear for rock joints.

Figure 17 indicates how the shear stress-displacement performance could be simulated using the JRC(mobilized) concept. For convenience, the gradients of the various loading, unloading and reversal curves are defined in units of m , which is given by the following empirical relation:

$$m = \frac{\phi_r/i}{0.3} \quad (5)$$

The denominator 0.3 is the value of $\delta/\delta(\text{peak})$ reached when dilation begins, as shown in Figure 16. Curve a.b.c.d.u. in Figure 17 follows the form of this figure. The unloading, reloading and reversal curves should be treated as guidelines at this stage. Celestino and Goodman's (1979) data were not obtained directly from rock joints, there was no weathering effect to stimulate gouge production, and the roughness of the surfaces was unusual, consisting of interlocking ripple marks molded from joints in sandstone.

The proposed method has been coded in the discrete element model UDEC, developed by Cundall (1980). Verification against future laboratory data is required. It is believed that the relevance of laboratory testing will be improved if a test device can be developed that allows accumulation of shear during successive cycles.

CONCLUSIONS

- Cyclic shear testing of rock joints at different frequencies, with equal forward and reverse components, may be relevant to the loading experienced by a stable rock mass. An unstable rock mass will tend to accumulate shear in the ultimate direction of failure, i.e. into a tunnel or open pit excavation.
- Instability under dynamic loading is enhanced when the joints concerned stand under combined shear and normal stress. Such a condition can be found when anisotropic principal stresses act on joints of different orientation than the principal stress trajectories. Potentially unstable conditions will also exist on certain joints that are intersected by a tunnel, if the unequal tangential and radial stresses result in a shear stress component along the joints in question. Joints dipping into a slope excavation will also have the potential to accumulate shear displacement under dynamic shaking.
- Severe seismic shaking has caused increased water flows into several mines, and joint slip, dilation and conductivity-enhancement in physical and numerical models of excavations in jointed rock.
- Such occurrences warrant consideration when designing water transport tunnels and nuclear waste repositories below the ground water table. The eventual breaching of a repository will be greatly accelerated if joint conductivities increase due to a seismically induced slip. Persistent, inclined jointing and high values of differential stress are likely to accentuate such problems.
- Tunnel support and rock mass reinforcement strategies in seismically active regions should incorporate the use of thin flexible liners of fiber-reinforced shotcrete and systematic rock bolting, to increase the modulus of the surrounding ground. A design giving flexibility in the rock bolt system is advisable if extreme shaking is likely to cause joint slips of some millimeters or more. However, joint conductivity may be expected to increase dramatically if joint slips of more than 2-3 mm occur.

- A dimensionless formulation of the shear strength-displacement behaviour of joints has been formulated using the mobilized roughness (JRC_{mob}) concept. This has been adapted to the formulation of dynamic loading of joints with shear reversal, and shear and damage accumulation.

REFERENCES

- BAKHITAR, K. and BARTON, N. (1984). Large scale static and dynamic friction experiments. Proc. 25th US Symp. Rock Mech., Evanstone, pp. 457-466.
- BANDIS, S., LUMSDEN, A.C. and BARTON, N. (1981). Experimental studies of scale effects on the shear behaviour of rock joints. Int. J. Rock Mech. Min. Sci. Geomech. Abstr. 18, No. 1, pp. 1-21.
- BANDIS, S., LUMSDEN, A.C. and BARTON, N. (1983). Fundamentals of rock joint deformation. Int. J. Rock Mech. Min. Sci. Geomech. Abstr. 20, pp. 249-268.
- BARTON, N. (1976). The shear strength of rock and rock joints. Int. J. Rock Mech. Min. Sci. and Geomech. Abstr. 13, pp. 255-279.
- BARTON, N. and CHOUBEY, V. (1977). The shear strength of rock joints in theory and practice. Rock Mechanics, Vol. 10, pp. 1-54.
- BARTON, N. and HANSTEEN, H. (1979). Very large span openings at shallow depth; deformation, magnitudes from jointed models and F.E. analysis. Proc. 4th Rapid Excavation and Tunneling Conf. Atlanta 2, pp. 1331-1353.
- BARTON, N. (1982). Modelling rock joint behaviour from in situ block tests: implications for nuclear waste repository design. Office of Nuclear Waste Isolation, OWNI-308, 96 p.
- BARTON, N. and BAKHITAR, K. (1984). Confidential report to Delft Hydraulic Laboratories, Terra Tek Engineering, Contract.
- BARTON, N., BANDIS, S. and BAKHITAR, K. (1985). Strength, deformation and conductivity coupling of rock joints. Int. J. Rock Mech. Min. Sci. Geomech. Abstr. 22, No. 3, pp. 121-140.
- BRACE, W.F. and BYERLEE, J.D. (1970). California Earthquakes: Why only shallow focus? Science, 168, pp. 1573-1575.
- BRACE, W.F. and JONES, A.H. (1971). Comparison of uniaxial deformation in shock and static loading of three rocks. Journal of Geophysical Research, Vol. 76, No. 20, pp. 4913-4921.

- BROWN, E.T. and HUDSON, J.A. (1974). Fatigue failure characteristics of some models of jointed rock. Earthquake Engineering and Structural Dynamics, Vol. 2, pp. 379-386.
- BYERLEE, J.D. and BRACE, W.F. (1968). Stick-slip, stable sliding, and earthquakes -- Effect of rock type, pressure, strain rate and stiffness. Journal of Geophysical Research, Vol. 73, pp. 6031-6037.
- CELESTINO, T.B. and GOODMAN, R.E. (1979). Path dependency of rough joints in bi-directional shearing. Proc. of the Fourth Int. Cong. on Rock Mech., Montreux, Vol. 1, pp. 91-98.
- CRAWFORD, A.M. and CURRAN, J.H. (1981). The influence of shear velocity on the frictional resistance of rock discontinuities. Int. J. Rock Mech. Min. Sci., Vol. 18, pp. 505-515.
- CUNDALL, P.A. (1980). A generalized distinct element program for modelling jointed rock. Report PCAR-1-80, Contract DAJA37-79-C-0548. European Research Office, US Army. Peter Cundall Associates.
- DIETERICH, J.H. (1972). Time-dependent friction in rocks. J. Geophys. Res. Vol. 77, No. 20, pp. 3690-3697.
- DOWDING, C.H. and ROZEN, A. (1978). Damage to rock tunnels from earthquake shaking. J. Geotech. Eng. Div. 104 (GT2), pp. 175-192.
- GILLETTE, D.R., STURE, S. and KO, H.-Y. (1983). Dynamic behaviour of rock joints. Proc. 24th U.S. Symp. on Rock Mech. Texas A & M University.
- GREEN, S.J. and PERKINS, R.D. (1968). Uniaxial compression tests at varying strain rates on three geologic materials. 10th U.S. Symp. on Rock Mech., University of Texas, Austin.
- HOSKINS, E.R., JAEGER, J.C. and ROSENGREN, K.J. (1968). A medium-scale direct friction experiment. Int. J. Rock Mech. Min. Sci., Vol. 5, pp. 143-154.
- KUTTER, H.K. and WEISSBACH, G. (1980). Der Einfluss von Verformungs- und Belastungsgeschichte auf den Scherwiderstand von Gesteinskluftun unter besonderer Berücksichtigung der Mylonitbildung. Final report of DFG research project Ku 361/2/4.
- MARTIN, G.R. and MILLAR, P.J. (1974). Joint strength characteristics of a weathered rock. Proc. of the 3rd Int. Cong. on Rock Mech., Denver, Colorado, Vol. 2A, pp. 263-270.
- McCLURE, C.R. (1982). Damage to underground structures during earthquakes. Proc. Workshop Seismic Performance of Underground Facilities, Augusta, pp. 75-106.
- PLESHA, M.E. and HAIMSON, B.C. (1988). An advanced model for rock joint behaviour: analytical, experimental and implementational considerations. Key Questions in Rock Mechanics, Ed. Cundall et al., Proc. 29th U.S. Symp. on Rock Mech., Minnesota, USA, pp. 119-126.
- ROVETTO, R. (1984). Private communication.
- SCHWARTZ, C.W. and KOLLURU, S. (1982). The influence of stress level on the creep of unfilled rock joints. Proc. of 23rd U.S. Symp. on Rock Mech., Univ. of California, Berkeley, pp. 333-340.
- STEVENS, P.R. (1977). A review of the effects of earthquakes on underground mines. Open-File Report 77-313. US Geological Survey.
- WEISSBACH, G. and KUTTER, H.K. (1978). The influence of stress and strain history on the shear strength of rock joints. Proc. of the 3rd Int. Cong. of Eng. Geologists, Madrid, Spain, Vol. II, 2, pp. 88-94.